Synergistic effect of calcium and magnesium on silica polymerization and colloidal silica fouling in bench-scale reverse osmosis filtration

Esmaeil Sarabian*, Greg Birkett, Steven Pratt

*School of Chemical Engineering (Andrew N. Liveris Building), The University of Queensland, St. Lucia, Queensland, Australia,
emails: e.sarabian@uq.edu.au (E. Sarabian), g.birkett@uq.edu.au (G. Birkett), s.pratt@uq.edu.au (S. Pratt)*

ABSTRACT

The main hardness cations, calcium and magnesium are prevalent in groundwater and brackish waters. Their effect on silica polymerization has been one of the main themes in the study of silica fouling and scaling in membrane filtration processes. However, their synergistic effect in real alkaline brackish waters (pH range of 8.5–9) at low concentrations (below 50 ppm of Ca and Mg), when total silica concentration reaches beyond solubility has not been well studied. Previous research, however, has been conducted on the effect of calcium, magnesium during reverse osmosis (RO) filtration showing that they have catalytic effect on silica polymerization, causing formation of more colloidal silica and at a faster rate. We investigated this effect by conducting bench-scale RO flat sheet experiments with and without calcium and magnesium, at mildly alkaline pH. The feedwater was RO concentrate collected from operating plants. The formed colloidal silica was characterised by monitoring its mass concentration during the fouling phenomenon and after collection of rejects at different recoveries, over a long period of time. In addition, colloidal silica morphology and elemental compositions were studied by scanning electron microscopy-energy-dispersive X-ray spectroscopy (SEM-EDS) analyses. Scaled membranes from both RO trials were also examined by SEM-EDS to study the scaling layer, along with elemental analysis of scales by inductively coupled plasma atomic emission spectroscopy. The results unequivocally emphasized the catalytic effect of calcium and magnesium by formation of higher amount of colloidal silica at a faster rate. This was confirmed by a significant amount of silica scales on the membrane surfaces from the trial with hard water.

Keywords: Colloidal silica; Reverse osmosis; Silicate scaling; Groundwater; Brackish water; Colloidal silica fouling; Effect of calcium and magnesium

1. Introduction

Silica has long been known to be one of the most prevalent scales on membrane filters during reverse osmosis (RO) desalination processes [1]. It can exist in three forms: monomeric silica or silicic acid $(Si(OH)_4)$, which is also known as dissolved or (molybdate)-reactive silica, colloidal or high molecular weight polymeric silicic acid, and lastly in the form of particulate silica which are large molecules usually in the form of clay, silt and sand [2]. Colloidal silica does not react with ammonium molybdate, hence they are also referred to as non-reactive or molybdate-unreactive silica [2].

It has been observed that colloidal silica can be formed through stages of RO desalination process from feed to the third stage [3]. In that study, Zaman et al. [3] conducted a set of experiments, measuring total and dissolved silica concentrations in coal seam gas (CSG) water from some water treatment plants (WTP) located in Queensland, Australia. CSG associated water is a type of brackish water extracted from CSG or coalbed methane production. The substantial

* Corresponding author.

increase in colloidal silica mass concentration remained an unanswered question by the study of Zaman et al. [3].

On the other hand, the role of calcium and magnesium on both silica polymerization and subsequently RO membrane performance were studied by many researchers; Braun et al. [4] and Hater et al. [5], and more recently Lu et al. [6]. While some conclusions are convergent, there are some inconclusive results in the literature. Crerar et al. [7] reported increased rate of silica polymerization in presence of 0.1 M of calcium and magnesium chloride, compared to sodium chloride (same concentration) in alkaline solution (pH 7 to 10.85). Sheikholeslami and Tan [8] have indicated that total hardness of the feed water to RO, would increase silica polymerization rate. However, this effect is negligible for low level of saturation or once the dissolved silica concentration drops to approximately 150 ppm. They demonstrated that magnesium had higher impact on silica polymerization rate. They also showed if this ratio is constant, increasing total hardness can increase silica polymerization rate. However, some of their results were found to be inconclusive. Also, polymerization rate in high silica (SiO_2 = 360 ppm) and low calcium (<100 ppm) concentration solutions seems to be decreasing [9] and was not further investigated even by other researchers. It should be noted that they did not observe gelation phenomenon of deposited colloidal silica that would over time cause a glassy region. It is not clear why glassy regions (which is known to be more detrimental) were not formed in their dynamic experiment. Therefore, the effect of calcium and magnesium, especially at lower concentrations, in naturally alkaline waters with complex matrices; such as coal seam gas (also known as coalbed methane) associated water warrants further investigation.

In this paper, we aimed to address the following research questions:

- Will colloidal silica form upon approaching the total silica concentrations of 250 mg/L (±5%) (as SiO_2) during RO filtration?
  - If formed, is there any difference in kinetics of polymerization and morphology of colloidal silica when comparing hard and soft waters?
  - Does the colloidal silica stay suspended in the bulk solution (reject stream) or does it cause membrane fouling? Are the results from hard and soft waters similar or different?

2. Materials and method

A very popular practice in RO membrane fouling and scaling research studies is RO flat sheet cell experiment. A once-through configuration would require a rig at pilot scale, where concentration factor (CF) is achieved by continuously discarding of permeate. Though ideal, it is not practicable with sample volumes available. A recycling configuration is commonly used to overcome this and is used here.

This configuration is a combination of rapid bench-scale membrane test (RBSMT) followed by batch recycle membrane test (BaReMT) for flat sheet membrane testing [10,11]. During RBSMT (the first phase), the permeate is discarded while the concentrate is recycled until a desired CF is achieved, afterwards, during BaReMT (the second phase), both permeate and concentrate streams are recycled to the feed tank [11]. The combined recycling stage, in some references, has been referred to as dynamic test [8]. The stage of combined recycling stage was maintained for 48 h. This decision was based on previous experience working with this type of brackish water RO concentrate and the setup's feed water tank volume. The rig was closely monitored during the concentrate recycling phase and liquid samples (from reject side) were collected at certain recoveries. Upon termination of concentration recycling, the system operated unmanned[1] during the combined cycling phase (next 48 h), as usually practiced by other researchers [12].

In this experiment, the target final CF was approximately 2. Once this CF is achieved, permeate and concentrate streams were combined and recycled back to feed according to BaReMT configuration (second phase). This exposes the membranes for a longer period to promote fouling.

The feed water was CSG RO concentrate to be fed at 55 bar (maximum allowable pressure). The initial flux was typical of SW flux at approximately 26 LMH. Experiments were run at constant pressure mode at fixed pressure of ~55 bar with a decrease in flux over time. At the end of the combined recycling or the second phase, the permeate flow-rates (in both trials) were dramatically dropped, exhibiting that the membranes were completely fouled. Membrane sheets were soaked in deionized (DI) water overnight. Then the compaction started and continues for the next 48 h. As per specifications, standard pre-made NaCl solution with concentration of 32,000 mg/L (as NaCl) with stable flux and the salt rejection within the upper end of the rejection for flat sheet, according to the membrane specification. Thereafter, the actual RO trial using real CSG RO concentrate s (original and softened) was started.

2.1. Feed water analysis

Samples in 20-L HDPE carboys were collected from a coal seam gas (CSG) operator WTP third stage reject stream. The analysis of water has been summarized in Table 1.

For the purpose of the second RO trial, 10 L of this water was softened by passing through a column packed by weakly acidic cation (WAC) ion-exchange (IX) resins. For this purpose, adequate volume of Purolite C104 Na-Plus (originally in sodium form) with an exchange capacity of 4.7 eq/L was placed inside a 1,000 mL Nalgene Imhoff polycarbonate settling cone (truncated cone). The original feedwater was slowly poured into the packed IX column and let pass through the resins in a batch mode. Further inductively coupled plasma atomic emission spectroscopy (ICP-OES) measurement of the collected effluent soften water, showed the concentrations of calcium and magnesium had dropped below detection limit.

2.2. RO configuration and setup

Two Sterlitech SEPA cells (installed in series with surface area of 140 cm^2, hence total surface area of 0.028 m^2) were assembled together with components of a typical

---

[1] Or minimal supervision

SEPA cell recycling test rig, shown in a schematic diagram. Fig. 1 left is a simplified block flow diagram of the rig used in this experiment and right is the photograph taken during the experiment.

Conductivity, pH, flow, pressure and temperature were monitored online. Calibration of conductivity probes was performed using 150 µS/cm standard solution for the permeate probe and 53,000 µS/cm standard solution for the feed probe. The pH probe was also calibrated with pH 7, pH 4 and pH 9 buffers. Table 2 summarizes the key

Table 1
Feed water for the 1st reverse osmosis trial

Element	Value
Ca, mg/L	11.5
Mg, mg/L	18.86
Na, mg/L	10,500
K, mg/L	55
NH_4, mg/L	4.5
Ba, mg/L	10.5
Sr, mg/L	18.4
CO_3, mg/L	285.4
HCO_3, mg/L	9,800
S, mg/L	3.2
Cl, mg/L	10,730
F, mg/L	26
NO_3, mg/L	0.35
P, mg/L	5.5
SiO_2 (total), mg/L	134.5
SiO_2 (dissolved), mg/L	134
SiO_2 (colloidal), mg/L	Negligible
B, mg/L	3.4
pH (lab-measured)	8.2
Conductivity (lab-measured), µS/cm	43,000
Ionic strength (calculated), M	0.5
Osmotic pressure (calculated), bar	22

operating parameters. The planned operation and conditions are virtually identical for trial 1 and 2.

2.3. Sampling (reject stream)

The concentrate stream was sampled by collecting 20 mL of the solution for every recovery point 10%, 20%, 30%, 40% and 50% (along with 100 mL of permeate stream, only to monitor performance and rejection). Three measurements were taken:

- Total silica and cations of interest; namely Na, Ca, Mg, (along with Al and Fe, if detectable) by ICP-OES.
- Dissolved silica by ammonium molybdate blue method (SMA blue).

At the end of the concentrate recycling phase, when the concentration factor of approximately 2 was achieved and the combined permeate and concentrate recycling phase was initiated, two more samples were collected 24 h apart.

2.4. Characterization of colloidal silica

Colloidal silica in reject samples were trapped on the filters of Amicon Ultra-4 (4 mL volume) centrifugal concentrators and spun at 5,000 rpm in Eppendorf Centrifuge 5804 R, for 10 min. This step was repeated multiple times followed by rising steps. The built-in filters of those concentrators were then extracted by scalpel, dried and coated with platinum. The specimen were, then, analysed by scanning electron microscopy (SEM) and energy-dispersive X-ray spectroscopy (EDS). This method is named ultrafiltration–ultracentrifugation or UF-UC and was only performed in those reject samples where there was a describable colloidal silica mass concentration (calculated by the differential technique).

2.5. Scaled membranes autopsy (morphology and elemental analyses of scaling species)

At the end of the experiment, the membrane sheets were extracted, and scalpel cut for autopsy and elemental profile
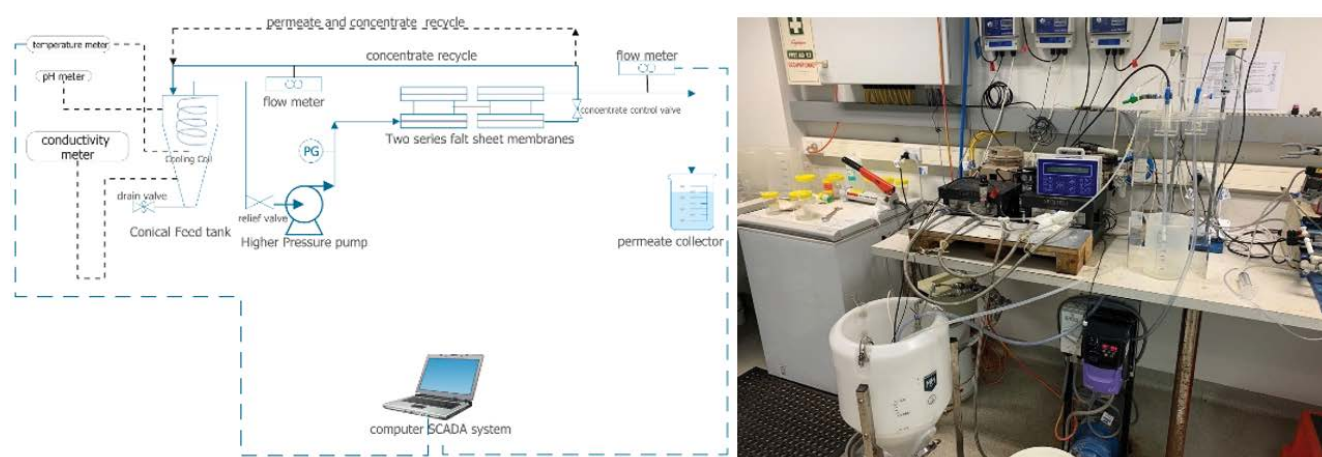

Fig. 1. Left: simplified block flow diagram of the current reverse osmosis test rig, showing recirculation lines, position of cells and online measurements; Right: a picture of the reverse osmosis test rig during the experiment.

Table 2
Key parameters for recirculation reverse osmosis trials

Parameter	Value
Cells used	2 × SEPA cells in series, Sterlitech SEPA cell
Cell area	2 × 140 cm^2, Sterlitech SEPA cell spec.
Membrane	DuPont FilmTec SW30
Cooling	Performed by stainless steel coil to maintain close-to-ambient temperatures
Initial feed water volume	10 L
Target concentration factor (CF)	~2
Permeate flowrate	13–16 mL/min (per cell)
Concentrate recirculation time	~7–8 h
Cell feed flowrate	1.5–1.8 L/min
HP pump feed applied pressure	55 bar

of scaling species. Displacement flush using DI water was performed to minimise the residue of feed water, and to suppress salt drying artefacts. The membrane sheets were kept in a Ziplock bag. To investigate irreversibility of the scales, the submerging in DI water was conducted overnight. This was to ensure that the excess amount of NaCl and possibly $CaCO_3$ were removed from the membrane surfaces so that these scales did not interfere with the SEM-EDS and ICP-OES analyses. The interference can occur when detecting the textural features of the colloidal silica, which can, in turn, interfere when detecting the EDS spectra of the more permanent foulants, if the scale's thickness is significant enough. Therefore, the following experiments were performed on the scaled membrane coupons.

2.6. Autopsy of scaled membranes

This autopsy was performed by drying in the clean room (after extraction of the scaled membranes immediately after termination of in-place rinsing) followed by SEM-EDS. This was to ensure all species were present and had not been removed by further washing.

- Further rinsed scaled membranes: To investigate irreversibility of silica scales, extended submerging in DI water, followed by drying and SEM-EDS analysis were performed. This was to remove more readily dissolvable solids and leave irreversible (difficult-to-dissolve) scaling species intact.

2.7. Elemental profile of scaling species

- All elements (expect silicon): A known area of the scaled membranes (along with same area of a virgin membrane, as control) were laid in a 50 mL tube containing 7% nitric acid and were left for 24 h. The solutions that contained scaling species were analysed by ICP-OES, similar to methods practiced by other researchers [13]. In this method, all sparingly soluble salts (including salts from drying but not silica), would have been captured.
- Silicon: NaOH pre-treatment to extract silica species (with and without prior overnight submerging in DI water), followed by ICP-OES.

2.8. Dissolved silica concentrations

Dissolved reactive silica concentration was measured by silicomolybdic heteropoly blue method (SMA blue) or the low range method. Based on that, Hach 8186 method was conducted according to Hach procedure adopted from Standard Methods [14,15]. Samples were diluted with Milli-Q deionized water to lower the expected concentration of silica to the working range concentration of the spectrophotometer (0.01–1.6 ppm). This dilution also meant that there was no significant physical interferences due to the sodium in solution [16,17]. The accuracy of the experiment was measured to be within approximately 5% relative error which is within the expected range of error (between 3% to 5%) published by Standard Methods [15].

2.9. Colloidal silica concentrations

It is a well-established technique to calculate mass concentration of colloidal silica by subtracting dissolved silica concentration (e.g., as SiO_2) measured by ammonium molybdate method from the total silica concentration (e.g., as SiO_2) measured by ICP-OES.

2.10. Total silica and other cations

Total silica (as SiO_2) and cations of interest such as sodium, calcium and magnesium were measured by (ICP-OES). The ICP instrument used was PerkinElmer Optima 8300DV. Samples were diluted with DI water to bring target ions into their measurement range and also to lower sodium concentration so that it did not cause any interference. Samples were then treated with nitric acid (HNO_3) as per Standard Methods [15]. No other pre-treatment and/or filtration was performed. The ICP-OES analysis had accuracy of approximately 7% (which was within the expected accuracy stated in the ICP manufacturer handbook [18]).

3. Results and discussion

Figs. 2 and 3 are two complied graphs that show data for hard and soft water, respectively. The key measure of membrane performance in this experiment is the flux trend, normalized for pressure and temperature. Each of
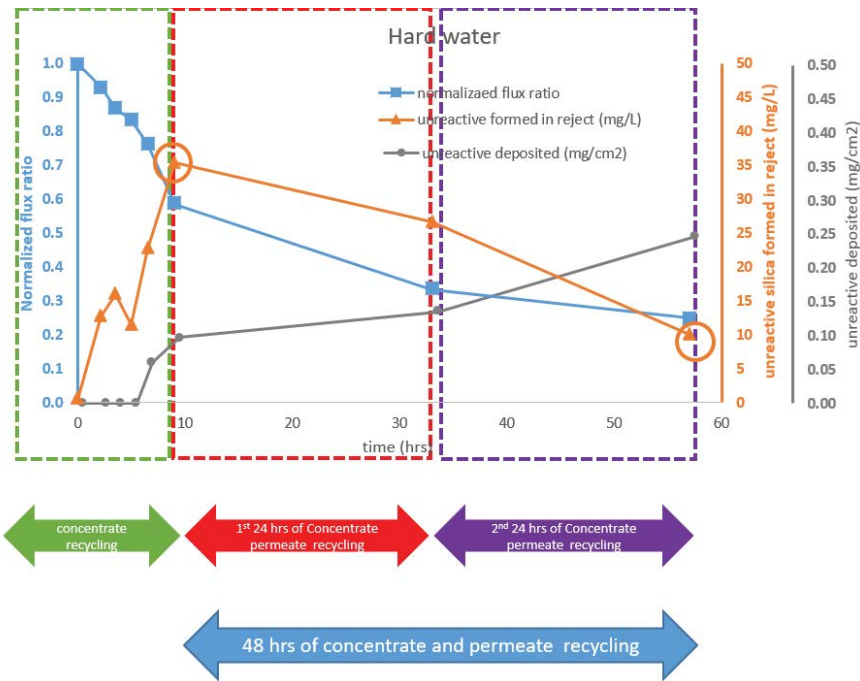
Fig. 2. Compilation graphs of normalized flux ratio (blue lines with square data points), colloidal silica in the reject (orange line with triangles) in mg/L and deposited (grey line with rounded dots) in mg/cm², during hard water trial.
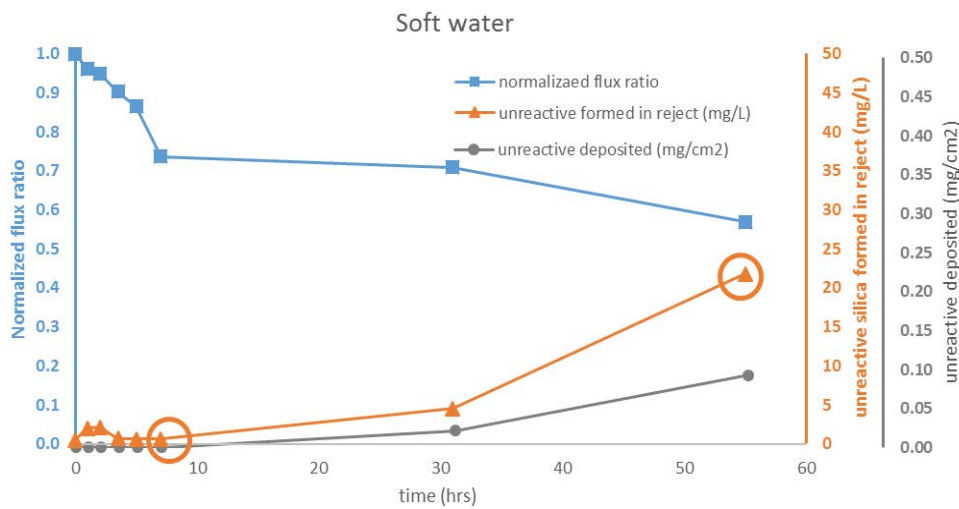

Fig. 3. Compilation graphs of normalized flux ratio (blue lines with square data points), colloidal silica in the reject (orange line with triangles) in mg/L and deposited (grey line with rounded dots) in mg/cm², during soft water trial.

these figures contains a blue line which is the normalized flux ratio, colloidal silica formed in the reject stream (the orange line) and colloidal silica deposited on the surface of the membrane (the grey line). The mass deposited (per surface area) was derived from the mass balance. Each line contains 8 data points. The first data point is the start of the trial, second until 5th points are data related to recoveries 10%, 20%, 30% and 40% and the 6th data point is the end of the first phase (recovery 50%), 7th is related to data 24 h after the start of the second phase and the last point is related to the end of the second phase, which is end of the experiment. The graphs are plotted against cumulative time in hours, and as illustrated in Fig. 2 the first phase, shown by green dotted box and double-headed arrow, is the first 9 h of concentrate recycling and the second phase is the next 48 h of combined recycling shown by red and purple dotted boxes and double-headed arrows.

Comparing these two graphs, it can be recognized that the initial flux decline (during 8–9 h of concentrate recycling phase) behaviours were similar. Membrane's performance running on hard water declined about 40%, while the membrane during soft water trail declined in its performance by

around 30%. This might point out that the onset of scaling in both cases were of similar nature. It is noticeable that the flux decline during the second stage of the experiment was more severe in the trial with hard water than in the trial with the soft water. This is one piece of evidence that membranes were more fouled (by silica species, as we will discuss later) in the first RO trial.

Colloidal silica mass concentration was calculated based on the difference of the total silica (as SiO_2) measured by ICP-OES and dissolved silica, measured by SMA blue method. As can be seen, the trend of colloidal silica formation was upward during the first stage of the trial with hard water and reached about 35 mg/L while the amount of formed colloidal silica during the same time in soft water trial is negligible. Thereafter, it is interesting to note that there is a decline in this type of silica species during the second phase in hard water trial, while this trend is slightly increasing during the trial with soft water. Even considering the errors associated with the colloidal silica calculation (Figs. 6–17), the loss of colloidal silica in hard water trial is a manifestation of deposition of silica on equipment's surfaces (including membrane surfaces). Therefore, the grey lines with rounded data points were expected trends that corresponds well with the trends of normalized flux ratio and colloidal silica formation in the last second phase of the trial (the 48 h of combined recycling phase). It should, however, be noted that the deposited mass per area, in both trials, were calculated to be very small values, relative to the colloidal silica mass concentration in reject stream.

3.1. Silica concentrations trends over time

The dissolved silica concentration in each collected sample were monitored over time to investigate polymerization kinetics. The dissolved silica concentration was measured by SMA blue method, every day for a period of about 10 d week (~230 h), to closely monitor the trend, and then over a longer period of time (maximum of approximately 60 d but at less frequency). For brevity, only result of two sample points are discussed here: end of the first and end of the second phase (as shown by circles in Figs. 2 and 3). Silica concentrations trends were plotted and shown in Figs. 4–7.

The orange dots are total silica (as SiO_2) measured by ICP-OES, while the blue vertical rhombuses denote dissolved or reactive silica, measured by SMA blue method. The grey dots illustrate calculated colloidal, while the green squares indicate estimated silica solubility at the measured pH, temperature, and estimated salinity. The error bars are associated with the corresponding experiment (ICP and SMA blue) and for the colloidal silica, it is the cumulative
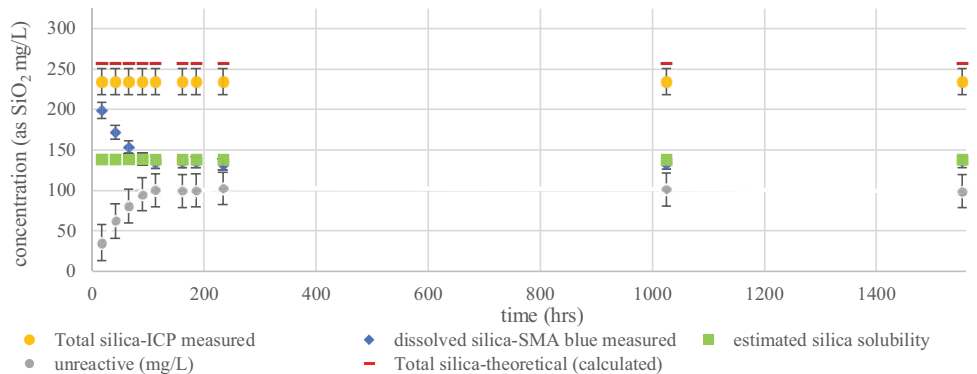
Fig. 4. Silica concentrations trend over time in the reject collected at the end of the first phase. Measured total and dissolved, calculated colloidal along with estimated silica solubility, in the trial with hard water.
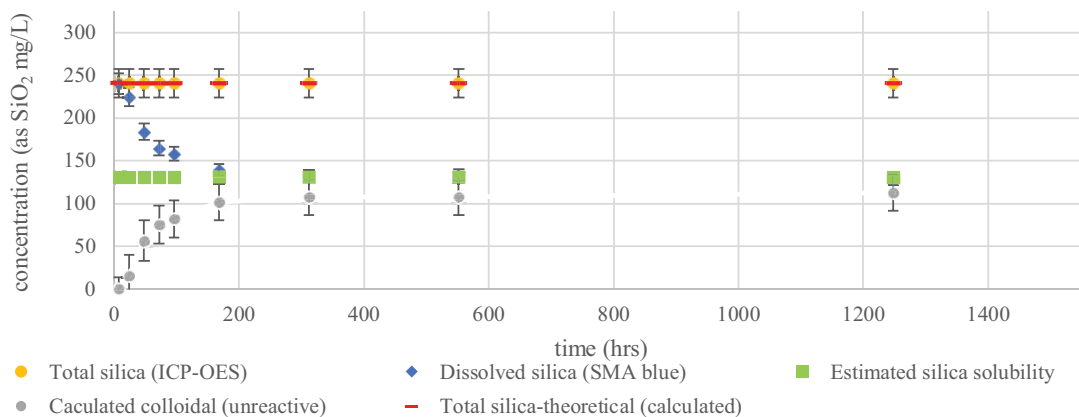
Fig. 5. Silica concentrations trend over time in the reject collected at the end of the first phase. Measured total and dissolved, calculated colloidal along with estimated silica solubility, in the trial with soft water.
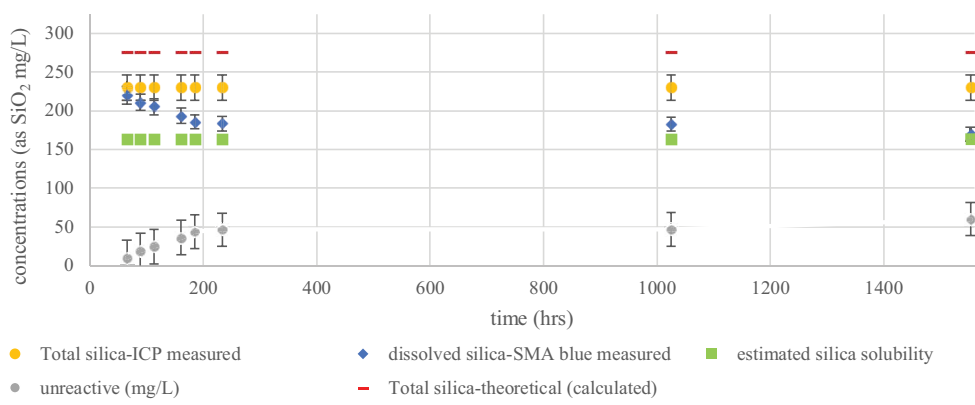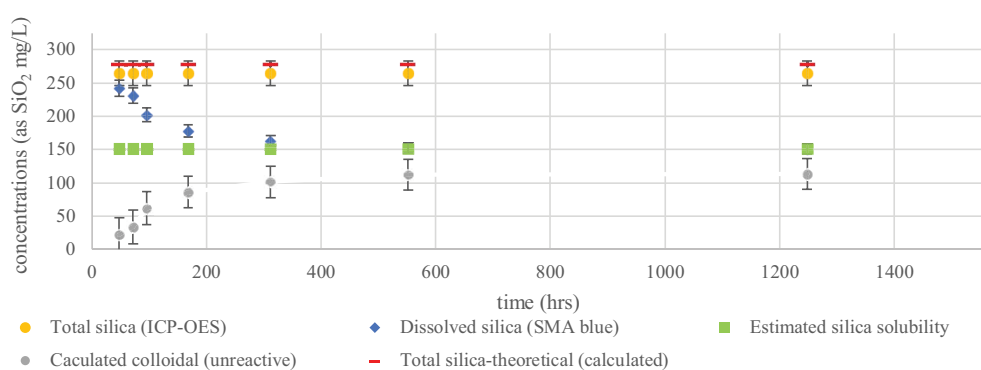
Fig. 6. Silica concentrations trend over time, at the end of the second phase. Measured total and dissolved, calculated colloidal along with estimated silica solubility, in the trial with hard water.

Fig. 7. Silica concentrations trend over time, at the end of the second phase. Measured total and dissolved, calculated colloidal along with estimated silica solubility, in the trial with soft water.

error associated with those two experiments. The term "initially" was used unequivocally for the first measurement of dissolved silica by SMA blue which occurred within the first 24 h of sample collection.

Figs. 4 and 5 show silica concentrations trends in the reject samples collected at the end of the first phase, by then a CF of approximately 2 was reached. It was observed that the theoretical (calculated) total silica concentration did not match the value measured by ICP-OES. The dashed line represents the expected total silica, labelled as theoretical (calculated) total silica in the graphs. As can be seen these dash lines are perfectly aligned with the ICP-measured total silica in the soft water, while in the hard water, there is a slight decrease in ICP-measured total silica (~234.5 mg/L measured, compared to ~258 mg/L expected total silica, as SiO_2). Since the error of ICP-OES has been considered, this ~23 mg/L difference in concentration might be explained by the loss of silica species due to deposition on surfaces, including membrane surfaces. This gap was widened in the next two samples of hard water.

In terms of the amount of colloidal silica formation and the achieved equilibrium, a more prominent difference between hard and soft water was observed. While 17% (of total) colloidal silica was initially formed in the hard water, this value increased sharply to about 40% in approximately 90 h, followed by stability of the dissolved silica concentration, in the soft water, insignificant amount of colloidal silica was initially formed with increase to about 42% after approximately 170 h, henceforth dissolved silica remained stable. Thus, it is obvious that the hard water sample reached equilibrium in a much faster manner.

Furthermore, comparing the graphs of silica concentration trends collected at different recoveries (where colloids were formed; at 30% and 40%) during the first phase with their corresponding points in the soft water (refer to the supplementary document), it can be understood that the concentration of silica decreased more rapidly, suggesting faster polymerization, as the final total silica concentration increased.

As can be seen in Figs. 6 and 7, the trends of silica concentrations in the last sample collected at the very end of the experiment (48 h after the start of the second phase) is interestingly different the previous sample points. Around 8% of colloidal silica species initially formed in the soft water sample, with an increase to 38% colloidal in about 300 h, reaching solubility after about 500 h, while in the hard water, the initial colloidal only made about 4% of the total silica, followed by an increase to only 20% within a comparable timeline, only approaching solubility after a much significant amount of time. We attributed this anomaly to the possible

change in silica equilibrium and meta-stability when significant amount of colloidal silica left the solution, during polymerisation and before the solution reaches equilibrium.

The loss of total silica in the hard water (the gap between the red bars and orange dots in Fig. 6) may not only be due to the membrane deposition, but also to other ancillary equipment's surfaces. Therefore, when calculating the deposited mass (of colloidal silica on membranes), the results from the accumulated silica mass derived from dissolving of scales on scaled membranes' surfaces would be more reliable. This matter is further discussed in the next sections.

3.2. Calcium and magnesium concentrations in rejects

The trend of calcium and magnesium concentrations in the collected samples are presented below. This is only applied to the first RO trial where the feed water contained calcium and magnesium. Fig. 8 shows the concentrations of calcium and magnesium measured by ICP-OES in the samples collected from the RO reject stream initially and at different recoveries during the first phase (10%, 20%, 30%, 40% and 50%) as well as two samples collected during the second phase.

Since calcium and magnesium did not precipitate during this experiment and remained in the reject solution, any effect of calcium and magnesium on silica polymerization is catalytic. As can be seen, both calcium and magnesium were concentrated by the expected CF through the first phase. In the samples collected during the second phase, a slight increase can be observed, which was possibly due to evaporation and water loss in the closed-loop system. Magnesium has exhibited pure catalytic role as reported by other researchers Lu et al. [6], Sheikholeslami and Tan [8], and Demadis et al. [19].

On the other hand, there was some insignificant loss of calcium during the second phase. Although Ca-induced colloidal silica fouling is reported by a few researchers (Lu et al. [6]), there is no evidence of calcium-induced silica scaling in these trials. The main evidence is that calcium was retained in the reject solution across different recoveries towards the end of the first cycle (concentrate recycling phase), while in the second phase, there is possibility that some calcium has been precipitated from the solution and deposited on the already scaled membranes' surfaces. This loss (~5 mg/L) could still be within the error of the ICP-OES experiment and EDS results were not consistent to re-confirm this.

Referring to graphs in Figs. 4 and 5 (as well as all other point in the first phase, provided in the supplementary section), it can be stated that the kinetics of polymerization are faster in the solution with calcium and magnesium. It should also be noted that in those monitored samples, the rate of silica polymerization is faster in presence of calcium and magnesium, as dissolved silica concentrations in those samples collected during the hard water reached estimated solubility faster. The relatively longer time to achieve equilibrium solubility in soft waters could be comparable to Sheikholeslami and Tan's results [8]. Overall, it can be stated that the difference in polymerization behaviour of hard and soft water can be attributed to the presence of calcium and magnesium.

3.3. Characterised colloidal silica in rejects

Based on the method described in the previous section, colloidal silica were trapped by UF-UC method, and then characterized by means of SEM-EDS for semi-quantitative elemental analysis. The following samples were subject to these analyses; reject samples collected at 50% recoveries (end of the first phase) as well as 24 and 48 h after the start of the second phase. In Figs. 9 and 10, micrographs of colloidal silica in the reject sample of hard and soft water collected at the end of the first phase (at approximately 50% recovery), along with the elemental profile are shown.

As can be seen, silicon has the highest atom percent in both samples, suggesting that the trapped colloids are silica-rich. In addition, morphometric features and average diameters of these colloids are similar in both samples. As can be observed, some of these colloids have turned into glassy areas in both samples. Therefore, it would be reasonable to claim that, overall, these results are comparable.
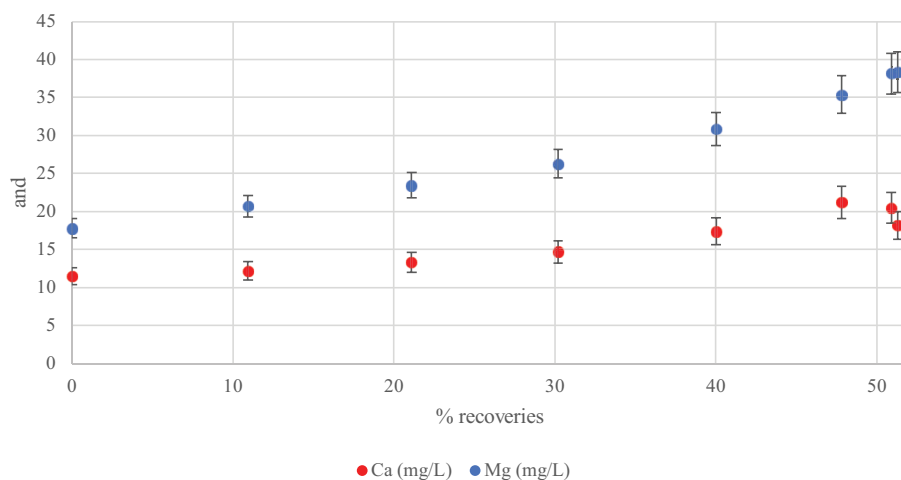

Fig. 8. Calcium and magnesium concentrations measured by ICP-OES in the collected rejects at different recoveries-in the trial with hard water.
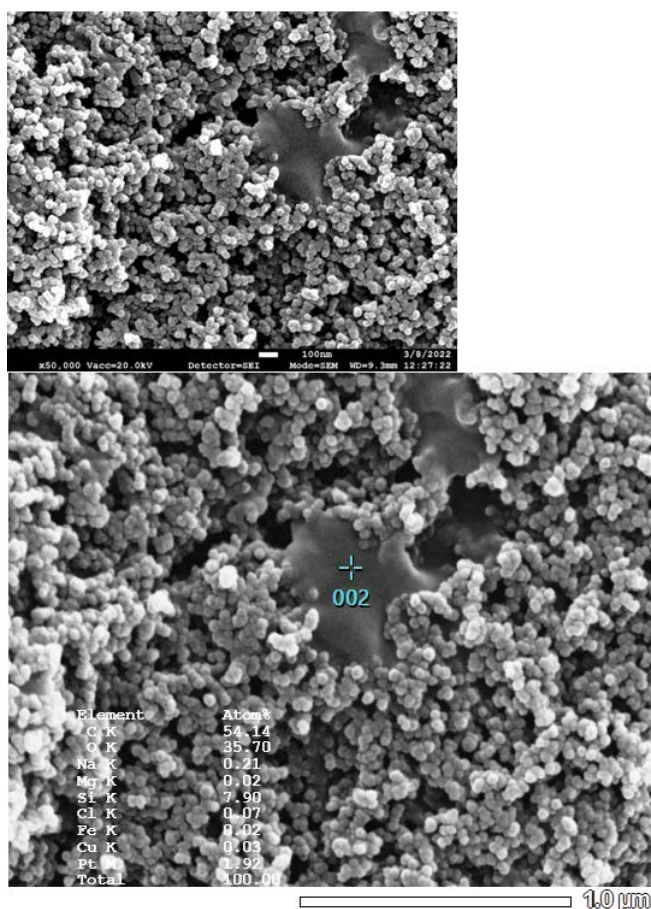
Fig. 9. Selected scanning electron microscopy micrographs of trapped silica colloids in reject of hard water at 50% recovery (end of first phase), inset in below picture in the elemental profile of the scanned area by EDS.

In Figs. 11 and 12 micrographs of silica colloids in the reject sample of hard and soft waters collected at the end of the second phase, along with the elemental profile are shown.

It appears that silica colloids in these samples have comparable features, in terms of size and morphology. Moreover, the difference between depth (thickness of the layer) and silicon peaks in these two samples are not appreciable.

Overall, grape-like silica-rich colloids were found in all samples, with no unusual or unexpected observation of irregular aggregated particles in both hard and soft water samples. Morphometrically, the detected silica colloids were very similar in both samples and their diameters were approximately 50 nm at the end of the first phase with some random increase in some particles at the end of the second phase. It would be challenging to ascertain the precise variety in diameters with these SEM micrographs, as it would require a proper particle size distribution technique. Silicon always had the highest peaks among spectra of other elements, while traces of aluminium, iron, sodium, chloride, copper, calcium and magnesium (for hard water and very occasionally in the soft water) were also occasionally detected. This was found to be possible residues of these elements in the solutions that were not removed after rinsing
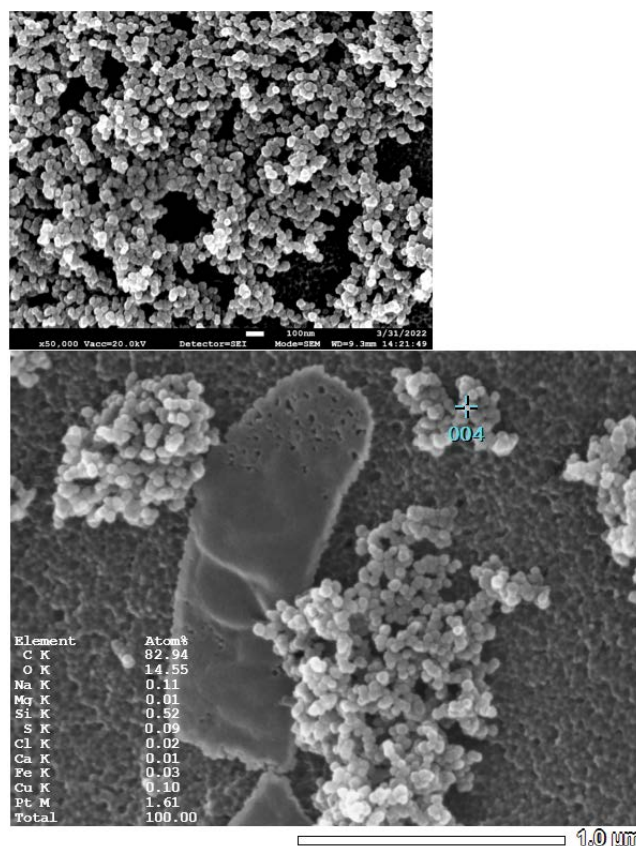

Fig. 10. Selected scanning electron microscopy micrographs of trapped silica colloids in reject of soft water at 50% recovery (end of first phase), inset in below picture in the elemental profile of the scanned area by EDS.

with DI water during the preparatory steps before SEM, and therefore is of insignificance.

3.4. Analysis of scaled membrane by autopsy (SEM-EDS)

Scaled membrane at the very end of the experiment were extracted as explained in the previous section. Two methods of autopsy on scaled membranes were performed to study the morphology of scales as well as elemental components of the scaling species:

- On extracted membrane at its original scaled status, and
- To investigate the irreversibility of the scaling, the same autopsy procedure after overnight submerging in DI water.

Two scan orientations were conducted: planar, and cross-sectional view. Figs. 13 and 14 show the top or planar view of the scaled membrane from the trial with hard and soft water, respectively. These pieces of scaled membranes were initially rinsed in place immediately upon termination of the experiment.

As can be seen, botryoidal silica-rich colloids, along with some glassy regions can be distinguished. Size of the colloids are similar in both trials and are of similar average diameter as those colloids characterized in the solution collected
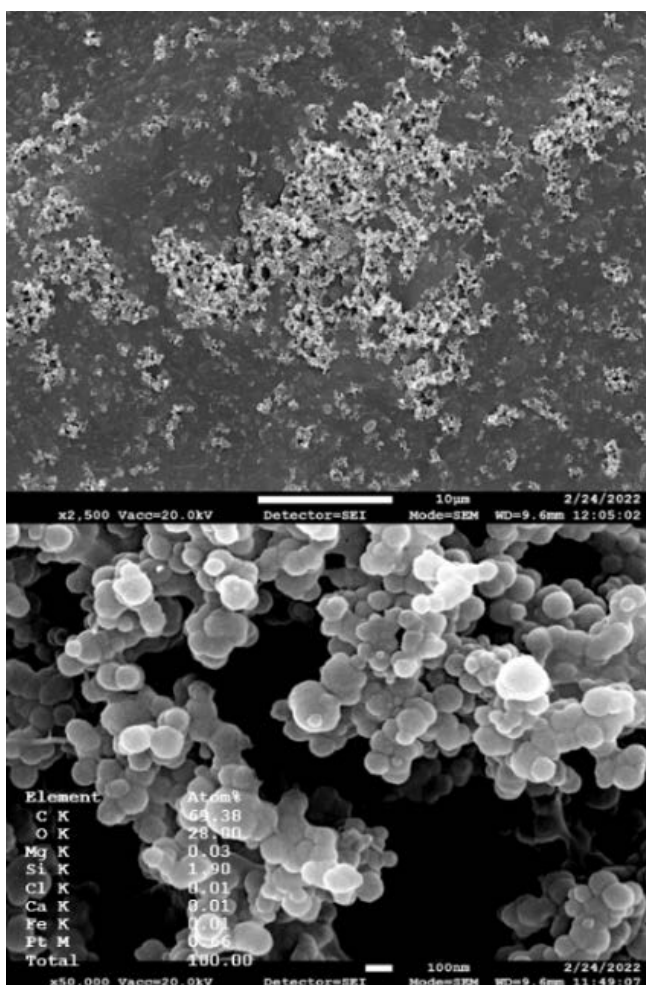
Fig. 11. Selected scanning electron microscopy micrographs of trapped silica colloids in reject of hard water at the end of the second phase, inset in below picture in the elemental profile of the scanned area by EDS.
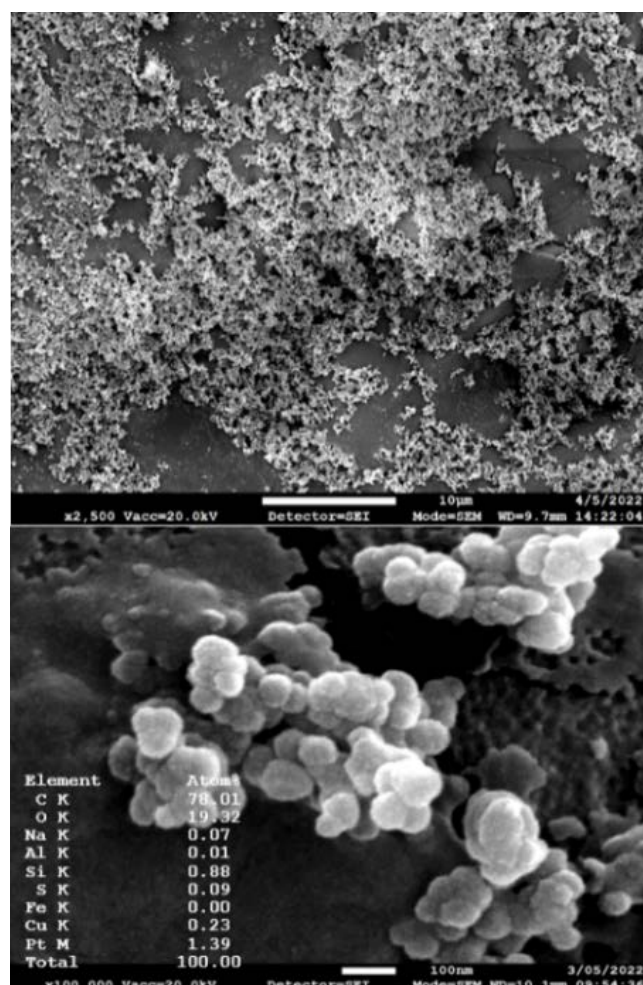

Fig. 12. Selected scanning electron microscopy micrographs of trapped silica colloids in reject of soft water at the end of the second phase, inset in below picture in the elemental profile of the scanned area by EDS.

at the end of the second phase (Figs. 9 and 10). Similar size of the colloids in the reject collected at the end of the trial and those deposited on the membrane, would suggest there were not significant growth or spherical polymerization on the surface of the membrane after colloids deposited on the surface of the membrane.

As expected, silicon is the most dominant element in EDS spectra for both samples and consistently across all scanned areas. Similar to the previous analyses, traces of calcium and magnesium, aluminium, iron, sodium, chloride and copper were also occasionally detected. Sulfur was detected occasionally when the scaling layer was thin enough (less than 120–150 nm), for electron beams to penetrate scaled membranes and reach the sulphur-rich polysulfone layer.

Overnight submerging in Milli-Q DI water yielded similar results; it did not remove silica colloids, neither did it remove the glassy regions. However, in EDS analysis of the scaled membrane from hard water trial, the mean silicon peaks (~13.3 in atom %) were almost halved (~6.6 in atom %). Such significant and consistent drop in silicon peaks was not found in EDS analysis of the submerged scaled membrane

from the soft water trial. This observation may suggest that there are some loosely adsorbed silica colloids on the top of the scaling layer of the membrane scaled during the hard water trial. This is while the trial with soft water has possibly resulted in a more irreversibly scaled membrane. These results are in line with results with the better quantifiable experiment (dissolving of scaling specie, followed by ICP-OES) and is discussed in the next section.

Cross-sectional SEM-EDS analyses was also performed, and similar results were obtained. Figs. 15 and 16 show the SEM images of scaled membranes in the trial with hard and soft water, respectively.

As expected and similar to the previous analysis, silicon is the most abundant element along with traces of calcium and magnesium, aluminium, iron, sodium, chloride and copper, in both specimens. A scaling layer of approximately 10 μm thickness can be distinguished. This layer is uneven, which makes comparison of the two surfaces difficult. In both specimens, the cauliflower-like scaled areas are of similar features with both rounded colloids and glassy regions that rich in silica.
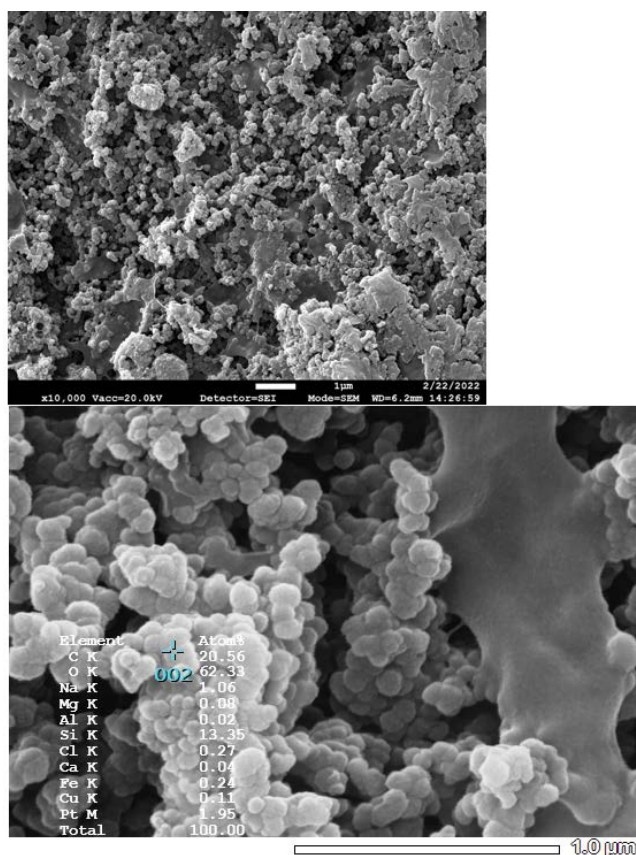
Fig. 13. Selected top view scanning electron microscopy micrographs of scaled membrane from the trial with hard water, inset in below picture in the elemental profile of the scanned area by EDS.
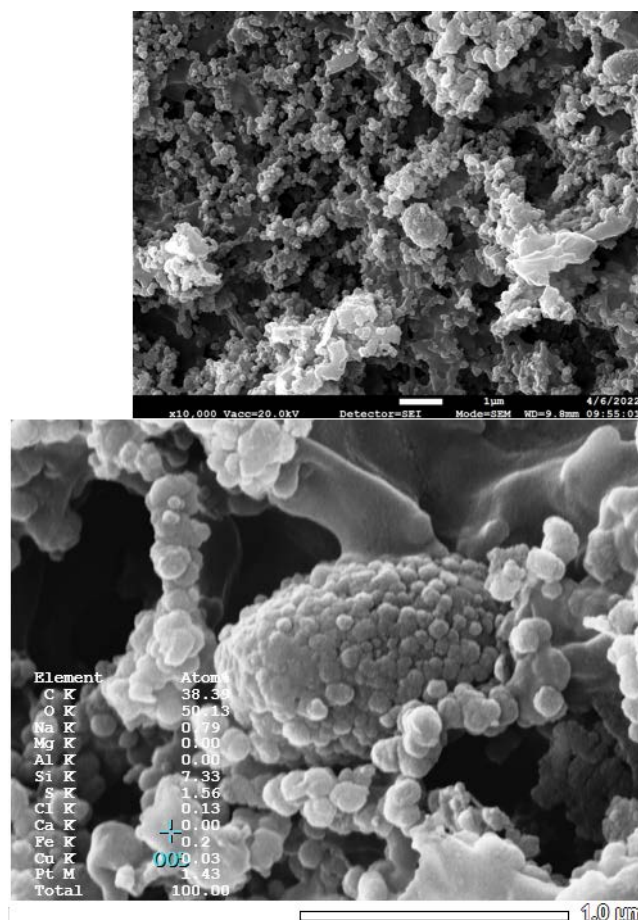

Fig. 14. Selected top view scanning electron microscopy micrographs of scaled membrane from the trial with soft water, inset in below picture in the elemental profile of the scanned area by EDS.

3.5. Analysis of scaled membrane: elemental profile of scaling species

To investigate the exact chemical make-up of scaling species (except for silicon), two dissolving experiments were conducted. A dissolving experiment was performed by submerging an extracted scaled membrane (from both RO trial) with total area of ~61.75 cm^2, in a 50 mL tube containing nitric acid of 7% concentration. A control was performed by cutting the same size of a virgin membrane undergoing the same treatment. Practical experience has shown that acid alone, would not be sufficient to dissolve amorphous polymeric silica scales, especially those glassy regions [20]. Therefore, another set of experiment was performed with a sodium hydroxide pre-treatment step (prior to ICP-OES) to ensure that the following ICP-OES would have measured all silica species. These two whole processes repeated with the scaled membranes submerged in DI water overnight. Based on the concentrations measured by ICP-OES, mass values were derived and summarized in Table 3. These values were estimated based on the assumptions that:

- Even distribution of deposition across the sheet.
- All silica scaling species were extracted from the sheet into the solution and measured by ICP-OES.

Insignificant amount (<LOR, once converted to deposited per area in mg/cm^2) of calcium and magnesium were detected on the scaled membrane from the hard water trial. Even those low values were not reported on the scaled membrane from the soft water trial. Other elements were found to be either below limit of detection (such as aluminium), within the error of ICP-OES, or erroneous, as they were also reported in the control specimen (virgin membrane of the same type and dimension), such as iron and sulphur. Along with silica, sodium was expectedly prevalent, due to highly saline RO feed water (both trials). The concentration of sodium was even expectedly higher, on those scaled membranes pre-treated by sodium hydroxide. In those cases, the concentrations of sodium reported on the NaOH-pretreated scaled membranes were aligned with the amount of NaOH used to perform the pre-treatment.

After 24 h of submerging in DI water, there was some reduction in silica. However, the percent reduction (~4.6%) in the scaled membrane from the soft water was not significant. A slightly higher reduction in the scaled membrane from the hard water, might be proof that some colloidal silica were loosely adsorbed on the outer layer of the scaling surface. This should be further investigated. Nevertheless,

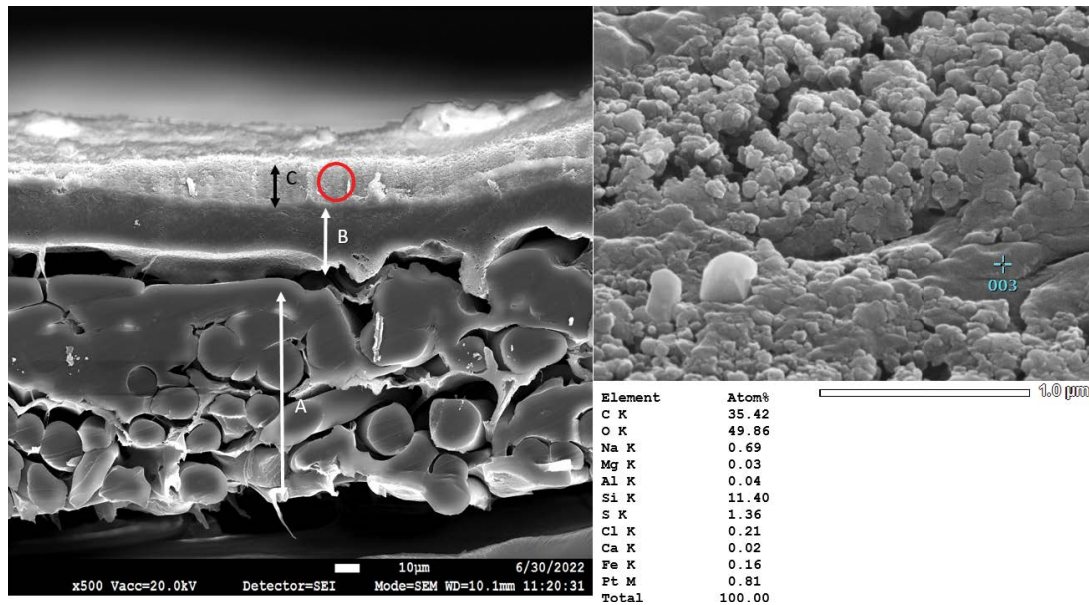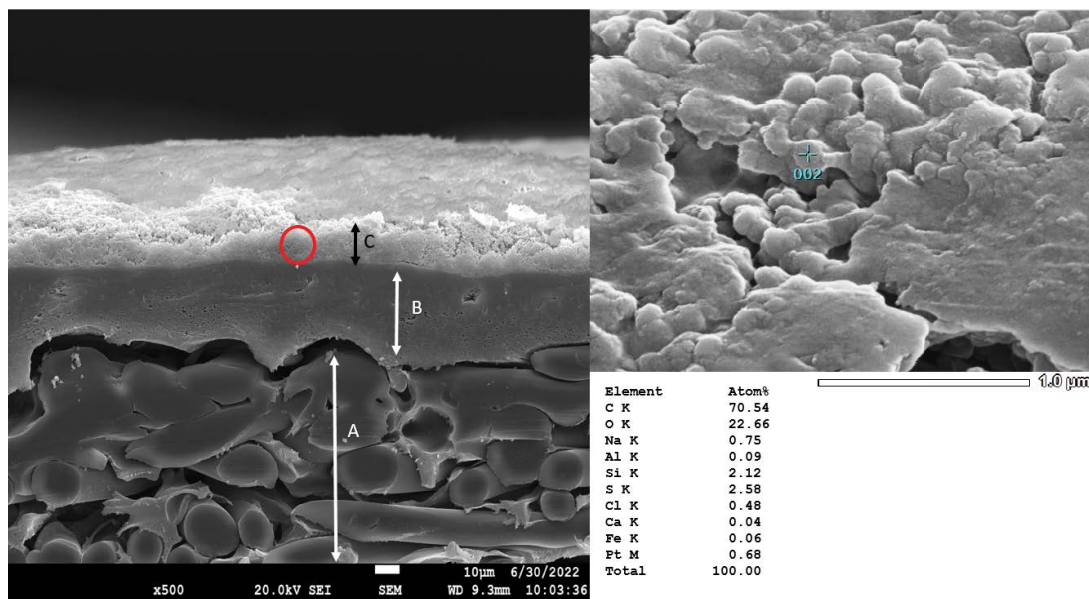| Element	Atom%
C K	35.42
O K	49.86
Na K	0.69
Mg K	0.03
Al K	0.04
Si K	11.40
S K	1.36
Cl K	0.21
Ca K	0.02
Fe K	0.16
Pt M	0.81
Total	100.00

Fig. 15. Left: a cross-sectional view scanning electron microscopy micrographs of scaled membrane from the trial with hard water. A is the reinforced fabric (polyester base), B is the polysulfone layer and C is scaling layer above the polyamide active layer (not shown). Right: the red circle in the left image is further magnified and the elemental profile of the scanned area by EDS, is shown under the image.

Element	Atom%
C K	70.54
O K	22.66
Na K	0.75
Al K	0.09
Si K	2.12
S K	2.58
Cl K	0.48
Ca K	0.04
Fe K	0.06
Pt M	0.68
Total	100.00

Fig. 16. Left: a cross-sectional view scanning electron microscopy micrographs of scaled membrane from the trial with soft water. A is the reinforced fabric (polyester base), B is the polysulfone layer and C is scaling layer above the polyamide active layer (not shown). Right: the red circle in the left image is further magnified and the elemental profile of the scanned area by EDS, is shown under the image.

results from this practice is another piece of evidence that show irreversibility of the silica scaling in both trials.

3.6. Possible scaling mechanism

A combination of events during both phases of recycling might have occurred and contributed to fouling pathway, therefore, the final scaling cannot be attributed to only one phenomenon. It is believed that in the first 8–9 h (concentrate recycling) fouling might have possibly initiated by pre-existing colloids and suspended solids in the solution that has caused comparable flux decline in both trials. Thereafter, it is believed, that further fouling was due to deposition of colloidal silica formed in the solution. This type of fouling

Table 3
Mass of elements deposited on the total area of both sheets (280 cm^2), per area, and percent reduction after submerging

RO trial	Element	Mass deposited on the scaled membrane (based on ICP-OES of digested scaled membrane) in total area 280 cm^2 (mg)	Mass deposited per area (mg/cm^2)	% decrease after overnight submerging in DI water
Hard water	Si (as SiO$_2$)	42	0.15	27.6%
	Ca	0.143	<LOR	<DL
	Mg	0.07	<LOR	<DL
Soft water	Si (as SiO$_2$)	22	0.08	4.6%
	Ca and Mg	<LOR	<LOR	N/A
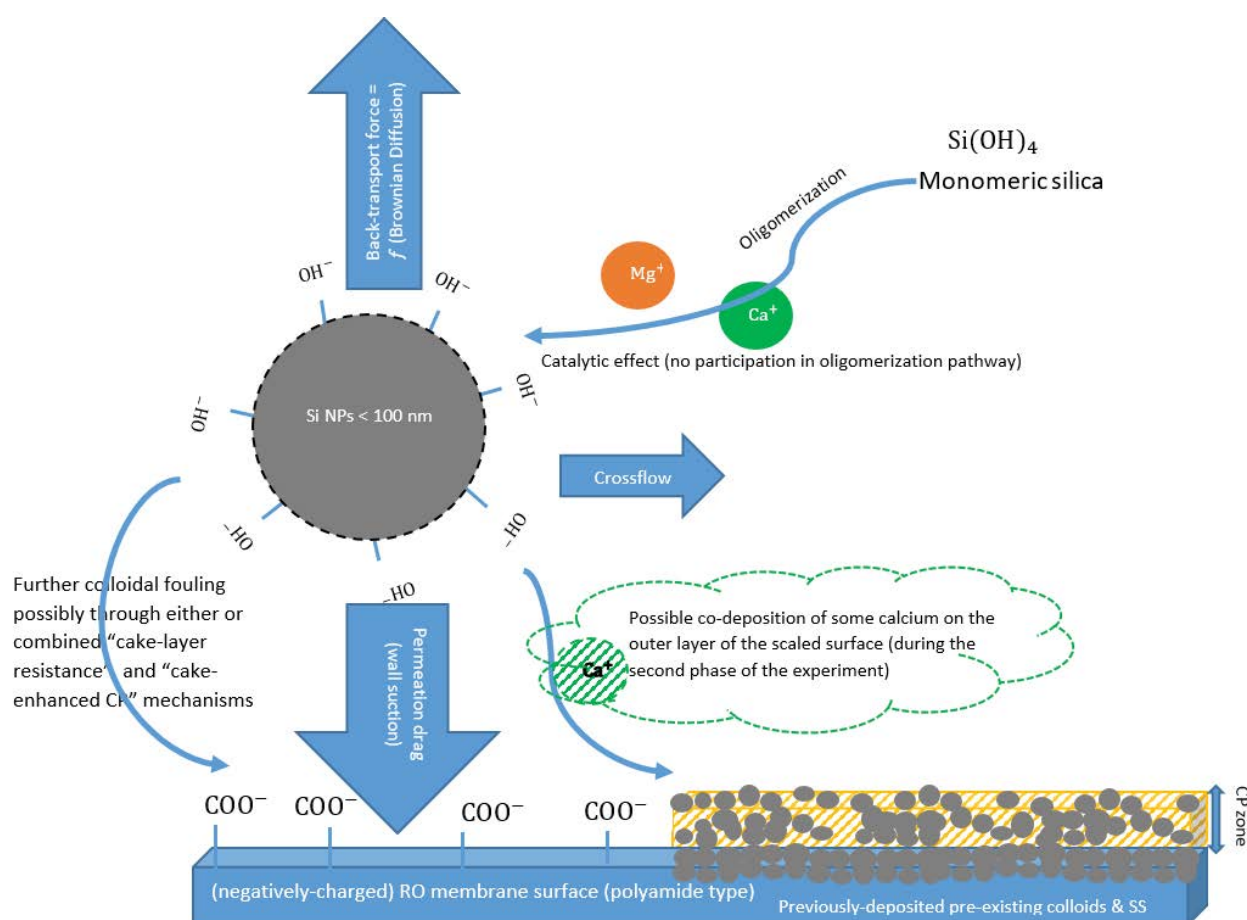
Fig. 17. Schematic of proposed colloidal silica fouling mechanism during the second phase (the last 48 h), more prominent in the hard water trial.

was initiated towards the end of the concentrate recycling stage, as colloidal silica mass concentration was increasing, but was more obvious, in the trial with hard water after 10 h towards the end of the experiment. It can be deduced that the significant normalized flux decline during the second phase was due to deposition of some of those colloidal silica formed in the solution. This possible phenomenon was manifested by loss of total silica concentration (compared to expected or theoretical values (Fig. 6). The colloidal silica deposition above the previously-formed scale could have been by either or combined mechanisms of cake layer resistance [21] and cake-enhanced concentration

polarization (CECP) [22]; both of which can aggravate the colloidal fouling mechanism and worsen the RO performance. Fig. 17 illustrates the deposition of the formed colloids on the pre-existing layer of scales, by cake layer resistance and/or CECP theories.

Glassy regions were most likely formed over time by gelation of previously deposited silica colloids and/or by addition of some monomeric silicates. This transition towards glassy region occurred in both trials, however it also warrants further investigation. It could be possible that the glassy area (as percent of the whole membrane's surface) in the trial with soft water was possibly more than the first trial

(shown difference in measured total silica concentrations of DI water overnight submerged membrane specimens, followed by ICP-OES when membrane specimens were pretreated by NaOH). It is possible that the top layer of the cauliflower area in the first trial contained loosely adsorbed colloidal silica on the outer surface of previously-fouled membrane surface.

4. Conclusion

Considerable amount of colloidal silica was formed during both trials with hard and soft water. However, it seems more colloidal silica was formed in the trial with hard water. In both trials the formation of colloidal silica in reject was associated with possibly irreversible silica scaling on membranes. Both calcium and magnesium were retained in the bulk solution which suggests that they have acted as catalytic ions and did not participate in the polymerization or deposition pathways. This feature is more highlighted for magnesium than calcium, supported by previous literature. Formation of colloidal silica was more pronounced in the hard water, and the kinetics of polymerization was faster in presence of calcium and magnesium. It should be noted that the presence of calcium in the collected rejects at different recoveries and at the end of first cycle may not prove calcium-induced silica fouling phenomenon suggested by Lu et al. [6]. However, since other scenarios could be possible, possible incorporation of calcium on the deposited scale warrants further trials with a variety of concentrations of calcium.

In summary, colloidal silica fouling was more severe in the trial with hard water proved by:

- A more rapid flux decline during the second phase of the trail;
- More colloidal silica on scaled membrane in autopsy (SEM images);
- An increased amount of silica (by alkaline pre-treatment and ICP-OES) from dissolving scaling species on scaled membranes surfaces.

In addition, since the size of the colloidal silica have not changed from the concentrate solution at the very end of the trial compared to the size of the deposited silica colloids, it can be claimed that there was not significant growth or spherical polymerization on the surface of the membranes after colloids deposited on the surface.

It should be noted that flat sheet RO cannot fully replace a once-through pilot-scale RO using spiral wound elements [5]. Experiments with flat sheet RO in recycling mode tends to produce more sever silica scaling; as reported by some researchers, this phenomenon can be exaggerated during such setup [23,24]. One reason for this could be the residence time that membrane sheets' surface area is exposed to fouling solution (silica-containing feed), which is much longer compared to the full-scale once-through spiral element configuration [23]. The other reason could be a relatively higher cross flow velocity on full scale RO which potentially causes less fouling and scaling on the spiral wound membrane surfaces [21,25].

References

[1] E.G. Darton, M. Fazell, A Statistical Review of 150 Membrane Autopsies, Presented at the 62nd Annual International Water Conference, Pittsburgh, October 2001, pp. 157–163.
[2] R.K. Iler, The Chemistry of Silica, John Wiley & Sons, Inc., United States of America, 1979.
[3] M. Zaman, G. Birkett, C. Pratt, B. Stuart, S. Pratt, Downstream processing of reverse osmosis brine: characterisation of potential scaling compounds, Water Res., 80 (2015) 227–234.
[4] G. Braun, W. Hater, C. Kolk, C. Dupoiron, T. Harrer, T. Götz, Investigations of silica scaling on reverse osmosis membranes, Desalination, 250 (2010) 982–984.
[5] W. Hater, C. Kolk, G. Braun, J. Jaworski, The performance of anti-scalants on silica-scaling in reverse osmosis plants, Desal. Water Treat., 51 (2012) 908–914.
[6] K.-G. Lu, M. Li, H. Huang, Silica scaling of reverse osmosis membranes preconditioned by natural organic matter, Sci. Total Environ., 746 (2020) 141178, doi: 10.1016/j.scitotenv.2020.141178.
[7] D.A. Crerar, E.V. Axtmann, R.C. Axtmann, Growth and ripening of silica polymers in aqueous solutions, Geochim. Cosmochim. Acta, 45 (1981) 1259–1266.
[8] R. Sheikholeslami, S. Tan, Effects of water quality on silica fouling of desalination plants, Desalination, 126 (1999) 267–280.
[9] R. Sheikholeslami, I.S. Al-Mutaz, T. Koo, A. Young, Pretreatment and the effect of cations and anions on prevention of silica fouling, Desalination, 139 (2001) 83–95.
[10] US Environmental Protection Agency (EPA), ICR Manual for Bench- and Pilot-Scale Treatment Studies, U.S. Environmental Protection Agency, 1996.
[11] F.A. DiGiano, S. Arweiler, J. Arthur Riddick Jr., Alternative tests for evaluating NF fouling, J. Am. Water Works Assn., 92 (2000) 103–115.
[12] R. Semiat, I. Sutzkover, D. Hasson, Scaling of RO membranes from silica supersaturated solutions, Desalination, 157 (2003) 169–191.
[13] G. Gonzalez-Gil, A.R. Behzad, A.S.F. Farinha, C. Zhao, S.S. Bucs, T. Nada, R. Das, T. Altmann, P.J. Buijs, J.S. Vrouwenveld, Clinical autopsy of a reverse osmosis membrane module, Front. Chem. Eng., 3 (2021) 683379, doi: 10.3389/fceng.2021.683379.

[14] Hach, Silica Heteropoly Blue Method, Hach Company, Loveland, Colorado, United States, 2014, pp. 1–6.

[15] R.B. Baird, A.D. Eaton, E.W. Rice, Standard Methods for the Examination of Water and Wastewater, L.L. Bridgewater, Ed., AWWA, APHA, WEF, Washington, D.C., 2017, pp. 1–1545.

[16] K.A. Fanning, M. Pilson, On the spectrophotometric determination of dissolved silica in natural waters, Anal. Chem., 45 (1973) 136–140.

[17] G.S. Bien, Salt effect correction in determining soluble silica in sea water by silicomolybdic acid method, Anal. Chem., 30 (1958) 1525–1526.

[18] C.B. Boss, K.J. Fredeen, Concepts, Instrumentation and Techniques in Inductively Coupled Plasma Optical Emission Spectrometry, PerkinElmer, Inc., USA, 2004.

[19] K.D. Demadis, A. Ketsetzi, E.-M. Sarigiannidou, Catalytic effect of magnesium ions on silicic acid polycondensation and inhibition strategies based on chelation, Ind. Eng. Chem. Res., 51 (2012) 9032–9040.

[20] K. Kezia, Personal Communications with Dr. Kezia Kezia (Wastewater Futures/Membrane Futures), 2021–2022.

[21] C.Y. Tang, T.H. Chong, A.G. Fane, Colloidal interactions and fouling of NF and RO membranes: a review, Adv. Colloid Interface Sci., 164 (2011) 126–143.

[22] E.M.V. Hoek, M. Elimelech, Cake-enhanced concentration polarization: a new fouling mechanism for salt-rejecting membranes, Environ. Sci. Technol., 37 (2003) 5581–5588.

[23] P. Sanciolo, N. Milne, K. Taylor, M. Mullet, S. Gray, Silica scale mitigation for high recovery reverse osmosis of groundwater for a mining process, Desalination, 340 (2014) 49–58.

[24] A.S. Gorzalski, O. Coronell, Fouling of nanofiltration membranes in full- and bench-scale systems treating groundwater containing silica, J. Membr. Sci., 468 (2014) 349–359.

[25] S. Jankhah, Hydrodynamic conditions in bench-scale membrane flow-cells used to mimic conditions present in full-scale spiral-wound elements, Membr. Technol., 2017 (2017) 7–13.

Supporting information

S1. Estimation of silica solubility

The solubility of silica has been estimated based on the equivalent salinity (from sodium chloride concentrations), pH of the solution and activity coefficient of non-ionic ortho-silicic acid as well as deprotonated ortho-silicic acid. The solubility of non-dissociated ortho-silicic acid was first predicted in DI water as per Fournier and Rowe [S1]:

$$\log C^*_{H_4SiO_4^0} = -\frac{731}{T} + 4.52 \tag{S1}$$

where $C^*_{H_4SiO_4^0}$ is the solubility of non-dissociated ortho-silicic acid in deionized water (in terms of mg/L of SiO_2 and T is temperature in Kelvin. Activity coefficient of non-dissociated ortho-silicic acid $\left(\gamma_{H_4SiO_4^0}\right)$ was calculated from Savenko's work by Eq. (S2) [S2]:

$$\gamma_{H_4SiO_4^0} = 1 + 0.0053S - 0.000034S^2 \tag{S2}$$

where S is salinity in terms of parts per thousand (g/L). Then, accounting for the above activity coefficient of non-dissociated ortho-silicic acid, the solubility of non-dissociated ortho-silicic acid was determined:

$$C_{H_4SiO_4^0} = \frac{C^*_{H_4SiO_4^0}}{\gamma_{H_4SiO_4^0}} \tag{S3}$$

where $C_{H_4SiO_4^0}$ is the solubility of non-dissociated ortho-silicic acid in salty solutions.

Since once dissolution from the solid phase to liquid phase occurs, only the first dissociation constant (K_1) of deprotonation reaction of ortho-silicic acid (to account for pH-dependent speciation) is important, which was, thereafter, determined using equation described by Fournier and Rowe [S1]:

$$\log K_1 = -\frac{2549}{T} - 15.36\left(10^{-6}\right)T^2 \tag{S4}$$

Lastly, the solubility was predicted using activity coefficients of both non-ionic and deprotonated ortho-silicic acid as well as K_1 and pH, described by Savenko [S2]:

$$C_{Si,total} = C_{H_4SiO_4^0} + C_{H_3SiO_4^-} = C_{H_4SiO_4^0}\left[1 + \frac{10^{pH} K_1 \gamma_{H_4SiO_4^0}}{\gamma_{H_3SiO_4^-}}\right] \tag{S5}$$

where $C_{Si,total}$ is the total predicted solubility of amorphous silica and $\gamma_{H_3SiO_4^-}$ is the activity coefficient of deprotonated ortho-silicic acid, calculated by using Davies equation, accounting for the solution ionic strength [S3]:

$$\log \gamma_i = -0.51z^2\left(\frac{\sqrt{I}}{1+\sqrt{I}} - 0.1I\right) \tag{S6}$$

S2. Silica concentration trends over time in rejects during the first phase

Figs. S1–S4 show the silica concentrations trends over time in the rejects, collected at 30% and 40% recoveries. For each set the first graph is related to the hard water and the second is the corresponding point in the trial with soft water. It is apparent that it took longer time for silica to reach its estimated solubility in the water that did not contain calcium and magnesium (the blue rhombuses reaching the green boxes).

S3. Autopsy scanning electron microscopy-energy-dispersive X-ray spectroscopy of scaled membranes after 24 h of submerging in DI water

Figs. S5 and S6 show the size and morphology of colloidal silica on the scaled membranes at the end of the reverse osmosis trial with the hard and soft water, respectively. The scaled membranes directly from the experiment were soaked in DI water for approximately 24 h prior to air drying and subsequent scanning electron microscopy-energy-dispersive X-ray spectroscopy (SEM-EDS). The EDS spectra repeatedly showed silicon to have the highest atom % along with traces of other elements. While there was not significant change in these spectra in analysing the scaled membrane from the soft water, the other specimen showed almost half of silica content than the other specimen analysed immediately after the experiment. These results were consistent with the dissolving of scaling specie, followed by ICP-OES (Table 3).
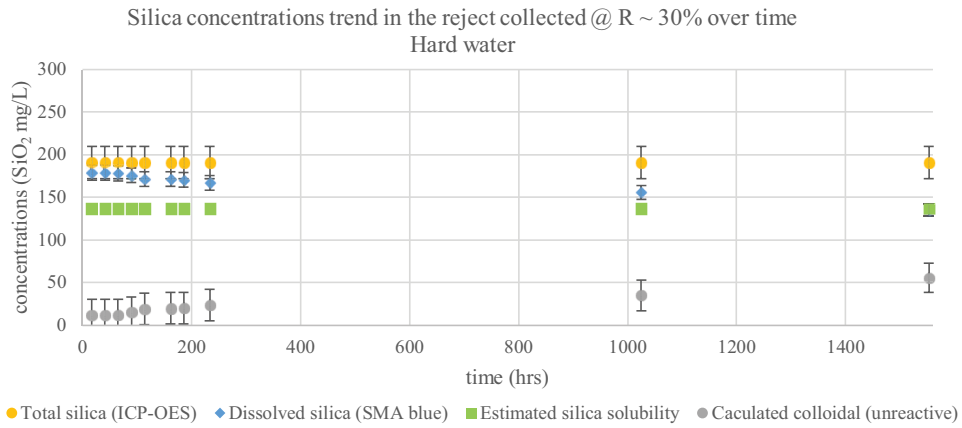
Fig. S1. Silica concentrations trend over time, in reject collected at 30% recovery. Measured total and dissolved, calculated colloidal along with estimated silica solubility, in the run with hard water.
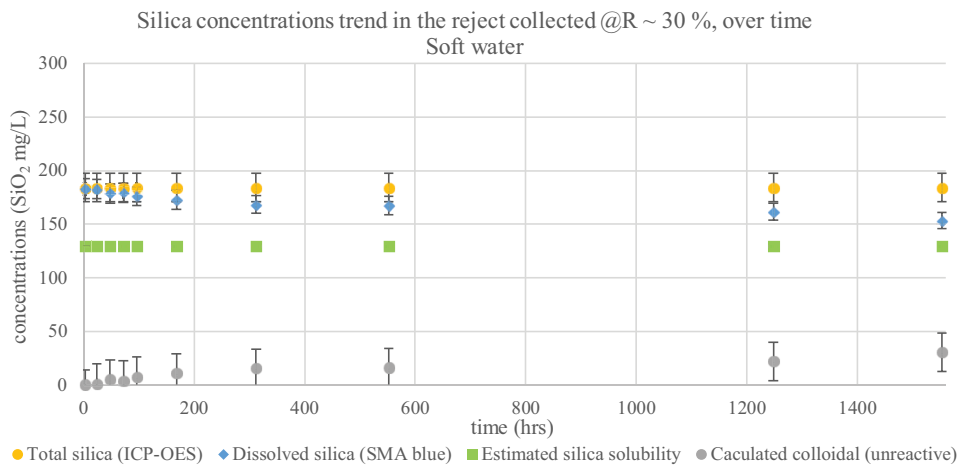

Fig. S2. Silica concentrations trend over time, in reject collected at 30% recovery. Measured total and dissolved, calculated colloidal along with estimated silica solubility, in the run with soft water.
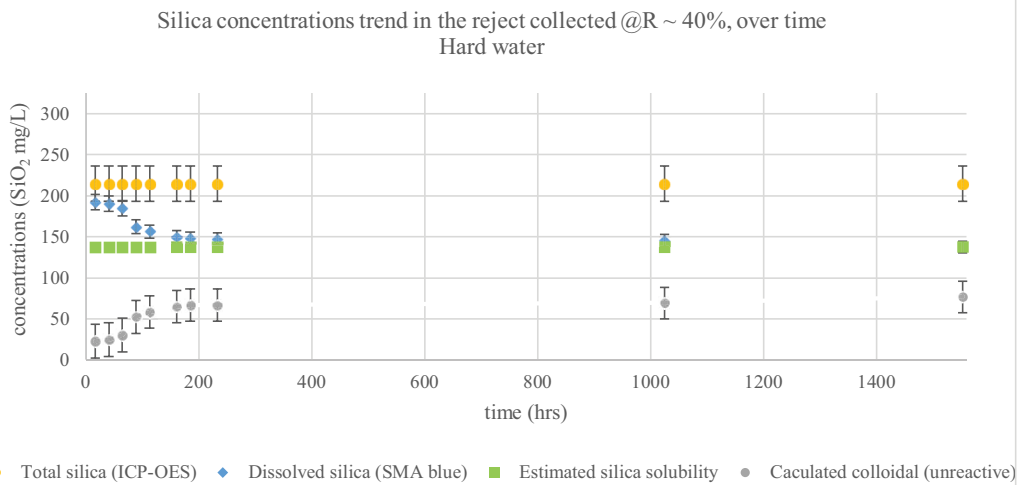

Fig. S3. Silica concentrations trend over time, in reject collected at 40% recovery. Measured total and dissolved, calculated colloidal along with estimated silica solubility, in the run with hard water.
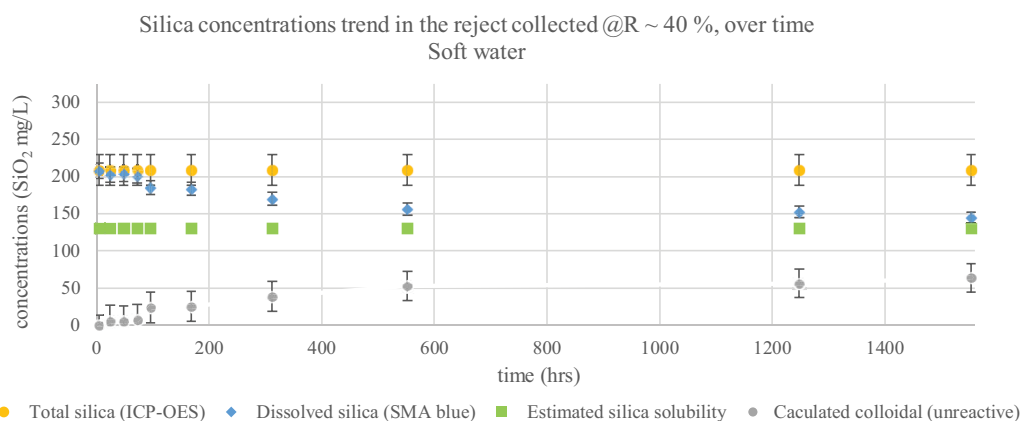
Fig. S4. Silica concentrations trend over time, in reject collected at 40% recovery. Measured total and dissolved, calculated colloidal along with estimated silica solubility, in the run with hard water.
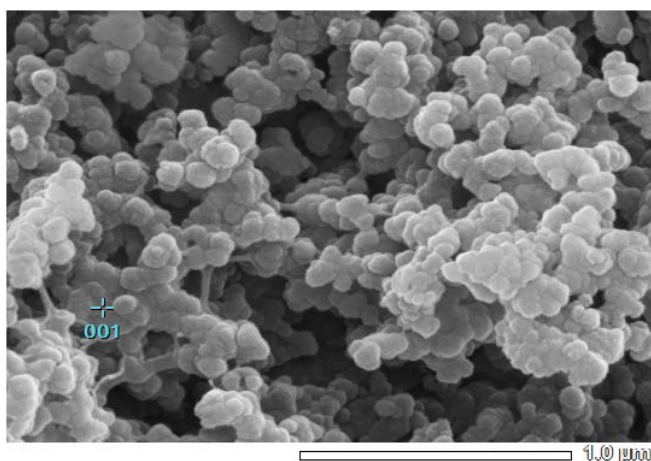

Fig. S5. Selected top view scanning electron microscopy micrographs of scaled membrane from the trial with hard water after overnight submerging in DI water, inset in below picture in the elemental profile of the scanned area by EDS.
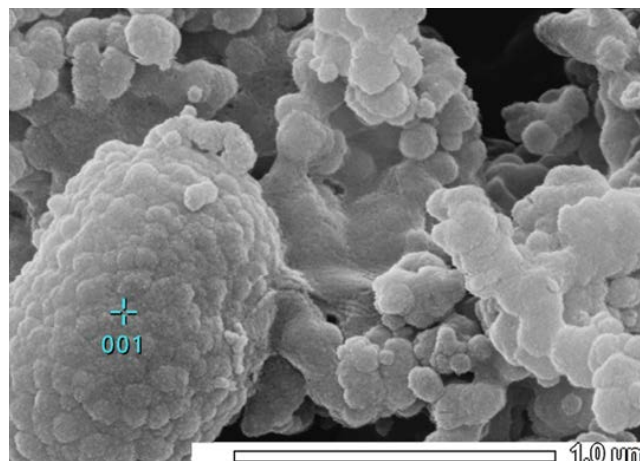

Fig. S6. Selected top view scanning electron microscopy micrographs of scaled membrane from the trial with soft water after overnight submerging in DI water, inset in below picture in the elemental profile of the scanned area by EDS.

References

S1. R.O. Fournier, J.J. Rowe, The solubility of amorphous silica in water at high temperatures and high pressures, Am. Mineral., 62 (1977) 1052–1056.

S2. A. Savenko, Experimental determination of the silica solubility and of the $H_4SiO_4^0$ activity ratio in standard and desalinated seawater, Oceanology, 54 (2014) 170–172.

S3. The Theoretical Interpretation of Chemical Potentials, Electrolyte Solutions, Chapter 9, Second Revised Edition, Dover Publications, USA, 2002.